

Contribution from the Departments of Chemistry and Biological Structure, University of Washington, Seattle, Washington 98195, and Department of Chemistry, Washington State University, Pullman, Washington 99164

Crystal Structure and Magnetic Behavior of $\text{Cu}(\text{C}_{14}\text{H}_{24}\text{N}_4)\text{CuCl}_4$: An Alternating-Metal-Site, Alternating-Exchange, Spin $1/2$ Linear-Chain System

Igor Vasilevsky,^{†,‡} Norman R. Rose,^{*‡} Ronald Stenkamp,[§] and Roger D. Willett^{*||}

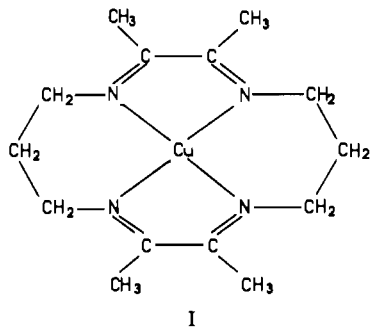
Received October 26, 1990

The crystal structure of the macrocyclic Cu(II) complex $\text{Cu}(\text{TIM})\text{CuCl}_4$ (TIM = 2,3,9,10-tetramethyl-1,3,8,10-tetraene-1,4,8,11-tetraazatetradecane) has been determined. The crystals, which are orthorhombic, space group $P2_12_1$ with $a = 8.086$ (2) Å, $b = 14.266$ (5) Å, $c = 17.544$ (2) Å, $V = 2024$ (1) Å³, and $\rho_{\text{calcd}} = 1.70$ g cm⁻³ ($Z = 4$), contain infinite chains running parallel to the c axis. The four-coordinate macrocyclic $\text{Cu}(\text{TIM})^{2+}$ cations are bridged by distorted tetrahedral CuCl_4^{2-} anions to form alternating $-(\text{Cu}(\text{TIM})-\text{CuCl}_4)_n$ chains. The cations thus achieve a distorted-square-bipyramidal geometry. The bridging of the CuCl_4^{2-} anion to adjacent $\text{Cu}(\text{TIM})^{2+}$ cations is asymmetric, leading also to alternating magnetic exchange pathways along the chain. Magnetic susceptibility measurements confirm the existence of two different exchange parameters: one ferromagnetic and one antiferromagnetic. Analysis of the data yields approximate values of $J_1/k = 13.3$ (4) K and $J_2/k = -2.6$ (1) K.

Introduction

The magnetic behavior of uniform spin $1/2$ Heisenberg chains has been well documented, for both ferromagnetic¹ and antiferromagnetic² magnetic exchange coupling. With the presence of a small spin anisotropy, the ferromagnetic chain has been shown to support nonlinear excitations called solitons.³ Dimerization of the chain leads to systems with alternating-exchange parameters, J_1 and J_2 .⁴ For a positive alternating parameter, $\alpha = J_2/J_1$, this system has been well studied.⁵ Of particular interest are systems where lattice forces are sufficiently soft to allow the dimerization to be driven by the exchange forces, causing the system to undergo a spin-Peierls transition.⁶ The case for $\alpha < 0$ produces an alternating ferro/antiferromagnetic system. These have not been as extensively investigated, and their study has been hampered by the lack of published theoretical models for analysis of the data.⁷

Much of the current interest in one-dimensional systems focuses on alternating-spin systems with antiferromagnetic exchange. This leads to a ferrimagnetic type behavior in the chain.⁸ One synthetic strategy for the rational synthesis of these types of systems involves the coupling of cations and anions containing different metal ions. In this paper, we present structural and magnetic studies on the homonuclear prototype of one such system, $\text{Cu}(\text{TIM})\text{CuCl}_4$, where the cation contains a Cu^{2+} ion constrained to a planar four-coordinate geometry by a tetradentate macrocycle, shown schematically as I, and the anion is capable of forming semicoordinate bonds to this macrocyclic complex.



Results

The structure contains mixed cation/anion chains, which run parallel to the c axis, as illustrated in Figure 1. The macrocyclic cation is nonplanar, due to the buckling of the six member CuN_2C_3 rings. The anion has a flattened tetrahedral coordination with trans angles of 129.3 (1) and 124.9 (1)°. Two of the chloride

ions form semicoordinate bonds to neighboring cations at distances of 2.676 (1) and 3.164 (1) Å. This gives the Cu(II) ion in the macrocyclic complex a distorted-square-bipyramidal geometry with unequal apical distances. This asymmetry is induced by the nonplanarity of the macrocycle and leads to the inequivalence of the two $\text{Cu}\cdots\text{Cl}-\text{Cu}$ linkages. Structural parameters of importance for the magnetic interaction through the Cl(2) and Cl(3) bridges are the $\text{Cu}(1)\cdots\text{Cl}(n)$ semicoordinate distances (3.164 and 2.676 Å for $n = 2$ and 3, respectively), the $\text{Cu}(1)\cdots\text{Cl}(n)-\text{Cu}(2)$ angles (122.0 and 115.8°, respectively), the $\text{N}(2)-\text{Cu}(1)-\text{Cl}(n)-\text{Cu}(2)$ torsional angles (-4.9 and 146.7°, respectively), and the dihedral angles between the CuN_4 and CuCl_4 planes (71.1 and 47.3°, respectively). No close contacts among atoms involved in the magnetic orbitals occur between adjacent chains. The closest $\text{Cl}\cdots\text{Cl}$ contacts are greater than 5.5 Å.

A plot of $\chi_M T$ vs T is shown in Figure 2. The gradual rise in $\chi_M T$ as the temperature initially decreases is characteristic of a magnetic system with a dominant ferromagnetic interaction, while the precipitous drop in $\chi_M T$ at low temperature indicates the presence of a weaker antiferromagnetic coupling. No maximum is observed in χ_M down to 4.2 K, so the value of the antiferromagnetic coupling is less than 3 K. With no significant interchain exchange pathway available, the two types of interactions must occur within the chain. Thus, one is associated with the Cl(2) bridging pathway and the other with the Cl(3) pathway. This defines an alternate chain system with $\alpha < 0$.

- (1) Johnson, J. D.; Bonner, J. C. *Phys. Rev. B* **1980**, *22*, 251. Groenendijk, H. A.; Blöte, H. W. J.; van Duynveldt, A. J.; Gaura, R. M.; Landee, C. P.; Willett, R. D. *Physics* **1981**, *106B*, 47. Kopinga, K.; Tinus, A. M. C.; de Jonge, W. J. M. *Phys. Rev. B* **1982**, *25*, 4685. Willett, R. D.; Landee, C. P. *J. Appl. Phys.* **1981**, *52*, 2004.
- (2) Müller, G.; Thomas, H.; Beck, H.; Bonner, J. C. *Phys. Rev. B* **1981**, *24*, 1429. Mohan, M.; Müller, G. *Phys. Rev. B* **1983**, *27*, 1776. Müller, G.; Thomas, H.; Beck, H.; Bonner, J. C. *Solid State Commun.* **1981**, *38*, 1.
- (3) Mikeska, H. J. *J. Phys. C* **1978**, *11*, 229; **1980**, *13*, 2913. Kopinga, K.; Tinus, A. M. C.; de Jonge, W. J. M. *Phys. Rev. B* **1984**, *29*, 2868. Kopinga, K.; Tinus, A. M. C.; de Jonge, W. J. M. *Phys. Rev. B* **1987**, *36*, 5398.
- (4) Duffy, W.; Barr, K. P. *Phys. Rev.* **1968**, *165*, 647. Bonner, J. C.; Blöte, W. M. J.; Johnson, J. D. *J. Appl. Phys.* **1979**, *50*, 7379. Hall, J. W.; Marsh, W. E.; Welles, R. R.; Hatfield, W. E. *Inorg. Chem.* **1981**, *20*, 1033.
- (5) Hatfield, W. E. *J. Appl. Phys.* **1981**, *52*, 1985. de Groot, H. M.; de Jongh, L. J.; Willett, R. D.; Reedijk, J. *J. Appl. Phys.* **1982**, *53*, 8238.
- (6) Bloch, D. *J. Phys. Chem. Solids* **1966**, *27*, 881. Moncton, D. E.; Birgeneau, R. J.; Interrante, L. V.; Wudl, F. *Phys. Rev. Lett.* **1977**, *39*, 507. van Bodegom, B.; Larson, B. C.; Mook, H. A. *B* **1981**, *24*, 150.
- (7) Chow, C.; Willett, R. D.; Gerstein, B. C. *Inorg. Chem.* **1975**, *14*, 205. O'Brien, S.; Gaura, R. M.; Landee, C. P.; Ramakrishna, B. L.; Willett, R. D. *Inorg. Chim. Acta* **1988**, *141*, 83.
- (8) Mosset, A.; Galy, J.; Coronado, E.; Drillon, M.; Beltram, D. *J. Am. Chem. Soc.* **1984**, *106*, 2864. Drillon, M.; Gianduzzo, J. C.; Georges, R. *Phys. Lett.* **1983**, *96A*, 1413. Caneschi, A.; Gatteschi, D.; Renard, J. P.; Rey, P.; Sessoli, R. *Inorg. Chem.* **1989**, *28*, 1976; **1989**, *28*, 3314.

[†] Deceased, April 30, 1989.

[‡] Department of Chemistry, University of Washington.

[§] Department of Biological Structure, University of Washington.

^{||} Washington State University.

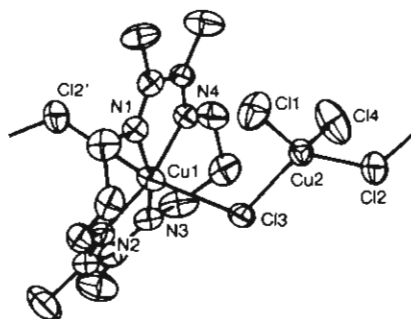


Figure 1. Thermal ellipsoid plot showing the chain structure.

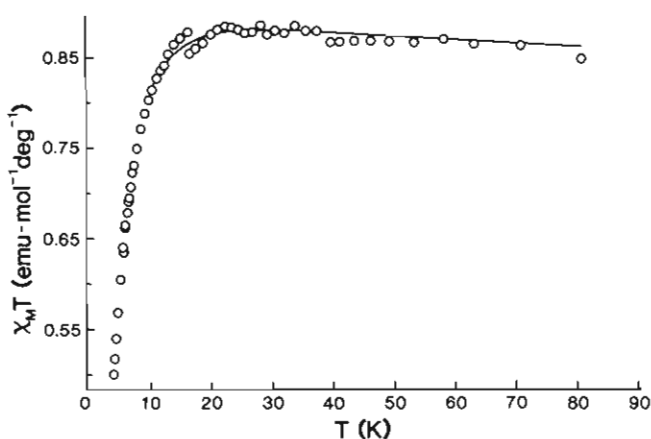
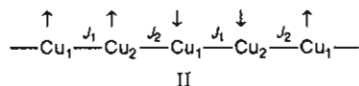


Figure 2. Plot of $\chi_M T$ vs. T . The solid line is the fit to the mean field corrected dimer model with $J_1/k = 13.3$ (4) K and $J_2/k = -2.6$ (1) K.

No expression is available in the literature for the susceptibility of such as alternating chain (II). However, with $|J_2| \ll |J_1|$, the

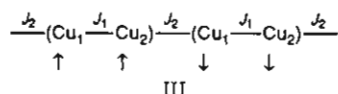


susceptibility can be approximated by using a mean field corrected dimer model with an interaction J_1 within the dimer and J_2 between dimers. Thus

$$\chi = \chi_{\text{dimer}} T / (T - \theta)$$

$$\chi_{\text{dimer}} = \frac{Ng^2\beta^2 S(S+1)}{3kT} \frac{3}{3 + \exp(-2J_1/kT)}$$

with $\theta = 2zJ_2/3k$ and $Z = 2$, the number of nearest neighbors of the dimers.⁹ The system is treated as a dimerized chain (III).



In the least-squares fit of the data, the value of g was fixed at 2.1 as determined from the high-temperature Curie-Weiss ($1/\chi$ vs T) plot. The solid line in the figures is for $J_1/k = 13.3$ (4) K and $\theta = 3.41$ (6) K. Only data for $T > 10$ K were included in the fit, since the mean field expression is only valid for $T \gg \theta$. The value of θ corresponds to $J_2/k = -2.56$ K, and thus the requirement $|J_1| > |J_2|$ is reasonably satisfied.

The existence of exchange coupling of opposite sign, despite structural pathways that are seemingly very similar, needs to be examined. In the cation, the unpaired electron lies in a $d_{x^2-y^2}$ σ -type orbital directed toward the nitrogen atom. For the compressed tetrahedral coordination of the anion, the magnetic orbital is a d_{xy} π -type orbital, using the conventional tetrahedral coordinate

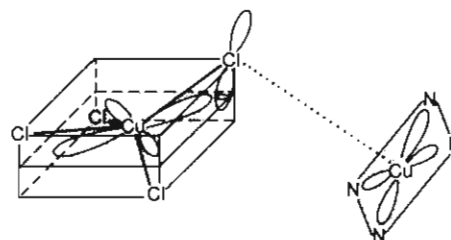


Figure 3. Diagrammatic illustration of the orbitals involved in the Cu-Cl...Cu superexchange pathway.

Table I. Crystallographic Data for Cu(TIM)CuCl₄

C ₁₄ H ₂₄ N ₄ Cl ₄ Cu ₂	space group: P2 ₁ 2 ₁ 2 ₁
fw = 512.24	$T = 22$ °C
$a = 8.086$ (2) Å	$\lambda = 0.71069$ Å
$b = 14.266$ (5) Å	$\rho_{\text{calcd}} = 1.70$ g cm ⁻³
$c = 17.544$ (2) Å	$\mu = 27.1$ cm ⁻¹
$V = 2024$ (1) Å ³	$R(F_o) = 0.043$
$Z = 4$	$R_w(F_o) = 0.037$

system (In the D_{4h} square-planar parentage, this is a $d_{x^2-y^2}$ orbital). The plane of this d_{xy} orbital will be approximately parallel to the least-squares plane through the CuCl_4^{2-} anion. The sign of the exchange coupling will depend upon the nature of the interaction of these two magnetic orbitals: orthogonality will lead to ferromagnetism; overlap will favor antiferromagnetism.¹⁰

The geometry of the magnetic orbitals is shown schematically in Figure 3. A π orbital on each chlorine atom in the CuCl_4^{2-} anion combines in an antibonding fashion with the d_{xy} orbital on Cu(2). The lower lobe of this orbital will point down toward the Cu(1)N₄ plane and interact with the $d_{x^2-y^2}$ -like antibonding orbital in that plane. For the Cl(2) bridge (the J_2 exchange pathway), where the N(2)-Cu(1)-Cl(2)-Cu(2) torsional angle is -4.9° , the π lobe is almost coplanar with one of the $d_{x^2-y^2}$ orbital lobes. Thus an antiferromagnetic interaction is predicted. Conversely, the corresponding torsional angle for the Cl(3) bridge (the J_1 exchange pathway) is 146.7° , so the lower lobe of the Cl(3) π orbital will lie in a plane nearly bisecting the lobes of $d_{x^2-y^2}$ -like orbital of the macrocycle. This will lead to near orthogonality and a ferromagnetic interaction. The much shorter length of the Cu(1)-Cl(3) distance, as compared to the Cu(1)-Cl(2) distance, is consistent with the observation that $J_1 > |J_2|$.

Experimental Section

Preparation. Crystals of the compound suitable for X-ray and magnetic studies were obtained by a diffusion technique. A 10-mL beaker with an acetonitrile solution of 0.34 g of $\text{CuCl}_2 \cdot 2\text{H}_2\text{O}$ (2.0 mmol) and 0.65 g of Et_4NCl (4.0 mmol) was placed in a 50 mL beaker. A 0.62-g (1.0-mmol, $x = 1$) amount of solid $\text{Cu}(\text{TIM}) \cdot x\text{H}_2\text{O}(\text{PF}_6)_2$ ¹¹ was placed in the annulus in the bottom of the 50-mL beaker, and acetonitrile was then slowly and carefully added to the 50-mL beaker until the lip of the smaller beaker was covered with approximately 0.5 cm of the solvent. At this point the mouth of the 50-mL beaker was covered with parafilm, and the nested beakers were allowed to sit at room temperature as dissolution of the $\text{Cu}(\text{TIM}) \cdot x\text{H}_2\text{O}(\text{PF}_6)_2$ and diffusion of the solutions took place. Over the course of several days, black prismatic crystals formed. The crystals were collected by filtration, washed with a small amount (about 2 mL) of acetonitrile, and air-dried. Yield: 0.435 g (84.1%). Anal. Calcd for $\text{C}_{14}\text{H}_{24}\text{N}_4\text{Cl}_4\text{Cu}_2$: C, 32.51; H, 4.68; N, 10.83; Cl, 27.42; Cu, 24.57. Found: C, 32.62; H, 4.69; N, 10.86; Cl, 27.62; Cu, 23.8.

Magnetic Measurements. The magnetic susceptibilities of powdered single crystals of the title compounds have been measured between 4.2 and 90 K in a PAR Model 155 vibrating-sampling magnetometer. The temperatures above 4.2 K were determined by using a carbon-glass resistance thermometer that had been calibrated in situ against a commercially calibrated diode and magnetic standards.¹² The magnetic field was measured by using a Hall probe. The susceptibilities per mole of

(9) Chow, C.; Willett, R. D.; Gerstein, B. C. *Inorg. Chem.* **1975**, *14*, 205.

(10) Kahn, O.; Briat, B. *J. Chem. Soc., Faraday Trans. 2* **1976**, *72*, 1441.
Girard, J. J.; Charlot, M. F.; Kahn, O. *Mol. Phys.* **1977**, *34*, 1063.
(11) Maroney, M. J.; Rose, N. *J. Inorg. Chem.* **1984**, *23*, 2252.
(12) Landee, C. P.; Greeney, R. E.; Lamas, A. L. *Rev. Sci. Instrum.* **1987**, *58*, 1957.

Table II. Fractional Coordinates, Estimated Standard Deviations, and Isotropic Temperature Factors for the Nonhydrogen Atoms in Cu(TIM)CuCl₄

atom	x	y	z	U, Å ²
C(1)	0.3178 (7)	-0.1804 (3)	0.3760 (4)	0.0579
C(2)	0.1381 (8)	-0.2096 (3)	0.3722 (3)	0.0584
C(3)	0.0296 (8)	-0.1701 (4)	0.4340 (3)	0.0540
C(4)	-0.0831 (6)	-0.0213 (4)	0.4696 (3)	0.0513
C(5)	-0.1884 (10)	-0.0570 (5)	0.5322 (4)	0.0927
C(6)	-0.0863 (7)	0.0838 (4)	0.4550 (3)	0.0491
C(7)	-0.1922 (9)	0.1451 (5)	0.5016 (4)	0.0831
C(8)	0.0266 (7)	0.2078 (3)	0.3786 (4)	0.0606
C(9)	0.1184 (8)	0.2180 (3)	0.3043 (3)	0.0572
C(10)	0.2983 (7)	0.1930 (3)	0.3046 (3)	0.0528
C(11)	0.4629 (6)	0.0539 (3)	0.3054 (3)	0.0382
C(12)	0.6113 (8)	0.1002 (4)	0.2728 (4)	0.0715
C(13)	0.4702 (7)	-0.0490 (3)	0.3274 (3)	0.0399
C(14)	0.6308 (7)	-0.0999 (4)	0.3188 (4)	0.0647
N(1)	0.3359 (5)	-0.0821 (2)	0.3515 (2)	0.0392
N(2)	0.0133 (6)	-0.0679 (3)	0.4281 (2)	0.0444
N(3)	0.0098 (5)	0.1089 (3)	0.4009 (2)	0.0419
N(4)	0.3256 (5)	0.0924 (2)	0.3186 (2)	0.0359
Cl(1)	0.3659 (2)	-0.1373 (1)	0.15505 (9)	0.0762
Cl(2)	0.1277 (2)	-0.0658 (1)	0.00592 (7)	0.0712
Cl(3)	0.01711 (15)	-0.02079 (9)	0.22646 (6)	0.0462
Cl(4)	0.2483 (3)	0.1315 (1)	0.10933 (9)	0.0890
Cu(1)	0.15655 (7)	0.00980 (3)	0.36255 (3)	0.0409
Cu(2)	0.19528 (7)	-0.02157 (4)	0.12360 (3)	0.0430

copper ions were corrected¹³ for diamagnetism (-128×10^{-6} emu/mol, Cl) and temperature-independent paramagnetism of the cupric ion ($+60 \times 10^{-6}$ emu/mol).

X-ray Data Collection. A black crystal of C₁₄H₂₄N₄Cl₄Cu₂ having approximate dimensions of $0.18 \times 0.27 \times 0.39$ mm was mounted on a glass fiber roughly along *b*. Cell constants and an orientation matrix for data collection were obtained, with Mo K α radiation ($\lambda = 0.71069$ Å) on an Enraf-Nonius CAD4 computer-controlled χ -axis diffractometer equipped with a graphite-crystal-incident-beam monochromator, by least-squares refinement of the setting angles of 25 reflections in the range $4 < \theta < 13^\circ$, measured by the computer-controlled diagonal-slit method of centering. The orthorhombic cell parameters and calculated volume are as follows: $a = 8.0857$ (16) Å, $b = 14.266$ (5) Å, $c = 17.5443$ (22) Å, and $V = 2024.3$ (14) Å³. With $Z = 4$ and a formula weight of 517.24, the calculated density is 1.70 g/cm³. The systematic absences unambiguously determined the $P2_12_12_1$ space group. A total of 3639 (3319 unique) reflections were collected at 23 ± 2 °C using ω - 2θ scans. An empirical absorption correction was applied based on a set of ψ scans ($\mu = 27.1$ cm⁻¹).

Structure Solution and Refinement. The structure was solved by using direct methods (RANTAN80).¹⁴ Hydrogen atom positions were calculated and used as fixed contributions to structure factor calculations. The structure was refined by full-matrix least-squares methods where the

(13) Selwood, P. W. *Magneto Chemistry*, 2nd ed.; Interscience: New York, 1956.

(14) Jia-Xing, Yao. *Acta Crystallogr.* **1981**, *A37*, 642.

Table III. Selected Bond Distances (Å) and Angles (deg) in Cu(TIM)CuCl₄

Bond Distances			
Cu(1)-N(1)	1.964 (4)	Cu(1)-Cl(2a) ^a	3.164 (2)
Cu(1)-N(2)	1.974 (4)	Cu(2)-Cl(1)	2.222 (2)
Cu(1)-N(3)	1.965 (4)	Cu(2)-Cl(2)	2.227 (1)
Cu(1)-N(4)	1.962 (4)	Cu(2)-Cl(3)	2.309 (1)
Cu(1)-Cl(3)	2.676 (1)	Cu(2)-Cl(4)	2.239 (2)
Bond Angles			
N(1)-Cu(1)-N(2)	96.7 (2)	Cl(1)-Cu(2)-Cl(2)	99.9 (1)
N(1)-Cu(1)-N(3)	163.7 (2)	Cl(1)-Cu(2)-Cl(3)	101.4 (1)
N(1)-Cu(1)-N(4)	81.2 (2)	Cl(1)-Cu(2)-Cl(4)	129.3 (1)
N(2)-Cu(1)-N(3)	81.4 (2)	Cl(2)-Cu(2)-Cl(3)	124.9 (1)
N(2)-Cu(1)-N(4)	167.2 (2)	Cl(2)-Cu(2)-Cl(4)	102.7 (1)
N(3)-Cu(1)-N(4)	97.1 (2)	Cl(3)-Cu(2)-Cl(4)	115.8 (1)
Cl(3)-Cu(1)-N(1)	96.6 (1)	Cu(1)-Cl(3)-Cu(2)	115.8 (1)
Cl(3)-Cu(1)-N(2)	100.4 (1)	Cu(2a)-Cl(2a)-Cu(1)	122.0 (1)
Cl(3)-Cu(1)-N(3)	99.7 (1)		
Cl(3)-Cu(1)-N(4)	92.4 (1)		

^aAn *a* denotes symmetry transformation by ($1/2 - x, -y, 1/2 + z$).

function minimized was $\sum w(|F_o| - |F_c|)^2$ and the weight w was defined as $4F_o^2/\sigma^2(F^2)$. Scattering factors were taken from Cromer and Mann^{15a} for non-hydrogen atoms and from Stewart et al.^{15b} for hydrogen. Anomalous dispersion effects were included,¹⁶ the values for f' and f'' were those of Cromer.¹⁷ The final cycle of refinement, with 217 parameters, converged (largest parameter shift was 0.01σ) with unweighted and weighted R factors of $R(F_o) = \sum ||F_o| - |F_c|| / \sum |F_o| = 0.043$ and $R_w(F_o) = [\sum w(|F_o| - |F_c|)^2 / \sum wF_o^2]^{1/2} = 0.037$ for 2951 reflections having intensities greater than 2σ . All calculations were performed on a VAX computer using XRAY76,¹⁸ except for placing of the hydrogen atoms, for which purpose the program CALCAT was used.¹⁹ A summary of pertinent crystal parameters is given in Table I. Atomic coordinates and equivalent isotropic thermal parameters are reported in Table II, while important interatomic distances and angles are given in Table III.

Note Added in Proof. A similar structure has been reported for [CuCy][CuCl₄]²⁻, where Cy = 1,4,8,11-tetraazacyclotetradecane.²⁰

Acknowledgment. Work was supported in part by NSF Grant DMR-8803382.

Supplementary Material Available: Tables of data collection and refinement parameters, anisotropic thermal parameters, hydrogen atom positions, torsion angles, least-squares planes, bond angles, and bond distances (10 pages); a table of observed and calculated structure factors (13 pages). Ordering information is given on any current masthead page.

(15) (a) Cromer, D. T.; Mann, J. *Acta Crystallogr.* **1968**, *A24*, 321. (b) Stewart, R. F.; Davidson, E. R.; Simpson, W. T. *J. Chem. Phys.* **1965**, *42*, 3175.

(16) Ibers, J. A.; Hamilton, W. C. *Acta Crystallogr.* **1964**, *17*, 781.

(17) Cromer, D. T. *International Tables for X-ray Crystallography*; The Kynoch Press: Birmingham, England, 1974; Vol. IV, Table 2.3.1.

(18) Stewart, J. M.; Machin, P. A.; Dickinson, C. W.; Ammon, H. L.; Heck, H.; Flack, H. *The X-ray System*; Tech. Rep. TR-446; Computer Science Center, University of Maryland: College Park, MO, 1976.

(19) Watenpugh, K. D. Private communication, 1972.

(20) Studer, M.; Riesen, A.; Kaden, T. A. *Helv. Chim. Acta* **1989**, *72*, 1253.